J Stat Phys (2009) 135: 935–950
DOI 10.1007/s10955-009-9743-z

Efficiency of Interacting Brownian Motors: Improved Mean-Field Treatment

František Slanina

Received: 22 November 2008 / Accepted: 15 April 2009 / Published online: 29 April 2009

Abstract The "reversible ratchet" model of interacting Brownian motors, introduced by us earlier, is investigated using a one-site approximation of a mean-field type. We confirm the effect of enhanced efficiency due to repulsive interaction and we provide arguments suggesting that the enhancement is of energetic, rather than entropic, origin. We also check the validity of the fluctuation theorem for stationary particle current.

Keywords Molecular motors · Fluctuation theorem · Exclusion process

1 Introduction

Brownian motors are one of paradigmatic realisations of driven non-equilibrium systems [1–13]. Besides the obvious relevance of their study for understanding the function of protein molecular motors [14–19], and practical realisations in nanotechnologies [20–22], they provide also an invaluable testing ground for fundamental questions of transport phenomena far from equilibrium [23].

In this paper, we focus our attention on two aspects of Brownian motors. The first one is their energetic efficiency, as expressed by usual thermodynamic definition $\eta = W/E_{\mathrm{in}}$, where W is work performed and E_{in} energy injected into the system from the outside. Other measures of efficiency, either those taking into account viscous resistance from the environment [24], those explicitly accounting for the consumption of chemical energy [25], or yet another ones, based on the magnitude of the stopping force [19], will be disregarded here. There are many studies investigating the efficiency of canonical Brownian motors realised as either flashing or rocking ratchets [26–34]. It turns out that the efficiency is rather low [8, 29], contrary to the experimental data on motor proteins, e.g. the kinesin [14, 19]. One is

F. Slanina (✉)
Institute of Physics, Academy of Sciences of the Czech Republic, Na Slovance 2, 18221 Praha, Czech Republic
e-mail: slanina@fzu.cz

lead to the natural conclusion that the usual ratchet mechanism with diffusion as principal driving force is not an appropriate model for biological motors.

Indeed, biologists distinguish between ratchet and power-stroke mechanisms for molecular motors [35], the later relying rather on quasi-deterministic downhill motion in a free-energy landscape which evolves in time. Thus, the particles move as if trapped in a travelling potential wave. This idea was elaborated in a toy model of "reversible ratchet" [32, 36, 37], showing much higher efficiency, close to the biologically relevant figures. We should note that high efficiency was also characteristic of the models of Refs. [25, 38].

The second point of interest will be the mutual repulsive interaction of several motors moving along the same track. Such situation is quite common in biological context. It was found [39–41] that in closed compartments, like in tubes representing the axons of neurons, the mutual steric (hard-core) repulsion of motors plays substantial role. The same holds for the movement of motors in complex arrays of cytoskeletal filaments [42]. Along the microtubules, kinesin molecules typically carry the cargo in groups [10, 11, 19]. If two types of motors move along the track in opposite directions, dynamical phase transitions may occur [43]. In gene transcription and translation large number of motor proteins move along the same track [44, 45], forming so-called "Christmas tree" structures. Strong interaction of hard-core type between individual motors plays decisive role in such situations. It was investigated on a model level for the transport of kinesin [46], ribosomes [47], and RNA polymerase [48]. Since the first investigations [39] these studies relied on ample literature on asymmetric exclusion processes [23, 49–51] and traffic models [52].

Including explicitly the ratchet mechanism of driven diffusion of hard-rod particles leads to very intricate effects [53–55], if the particle size and the ratchet periodicity are incommensurate. The collective movement of coupled Brownian motors was studied [56–58] and in some cases they were found to induce non-zero current and spontaneous oscillations even in mirror symmetric potential due to dynamical symmetry breaking [25, 59].

In our previous paper [60] we introduced a modified version of the "reversible ratchet". Spatial coordinate is discretised, as in e.g. [6]. Tunable on-site repulsion between particles is introduced. We found that not too strong interaction leads to increase of efficiency. The effect can be traced to decrease of the energy injected into the system, due to correlations between particle positions. While in [60] we relied on numerical simulations, in this paper we introduce an approximation which helps to study the system analytically. In essence, our approximation is a mean-field scheme. It is known that for the ASEP model mean-field approximation gives exactly some of the stationary-state averages, notably the average total current, which depends on density as $J_{\mathrm{tot}} = \rho(1 - \rho)$. We shall see that the ratchet current differs from this formula substantially. Let us also mention the mean-field treatment of motors which are coupled via a rigid backbone, as in the studies of spontaneous muscle oscillations [25, 59] or recently in [61]. In these works, the interaction of motors is effectively of infinite-range, due to the backbone, thus the mean-field treatment is close to be exact. Our case is different, because the interaction is on-site only. Therefore, we can expect only approximative results.

2 Interacting Particles in Reversible Ratchet

To investigate the effects of interaction on an energetic efficiency of motors, we chose a very schematic model, keeping deliberately only those ingredients which are necessary to show the effect. We realise that the cost to be paid for the schematicity is substantial loss of contact with the biological reality. On the other hand, we believe that the effects investigated

here are generic enough to be of value also for realistic modelling of molecular motors. We shall return to the important differences between our ratchet model and biological reality at appropriate places.

2.1 Time-Dependent Potential

Let us have N particles occupying, at time τ, integer positions $X_\tau = \{x_{i\tau}\}_{i=1}^N$, on the segment of length L, with periodic boundary conditions. The particles are subject to a periodic driving force, to the external load and they interact with other particles. Thus, the j-th particle moves in the potential

$$U_j(x,\tau) = V(x,\tau) + xF + gn_j(x,\tau). \tag{1}$$

The first term is spatio-temporally periodic external driving potential $V(x,\tau) = V_{x \bmod 3}(\tau) = V(x,\tau+4t)$. We chose the smallest non-trivial spatial period 3 for convenience, although larger periods may offer further interesting effects. The choice of period 3 is dictated by simplicity of the calculation. On the other hand, it was observed that the movement of myosin V molecules proceeds in three substeps within single period [62]. In reality, however, the substeps have unequal length, contrary to our model.

The time-dependent potential is periodic in space and time. It evolves in a four-stroke cycle. The full time period $4t$ is composed of four strokes of equal length t which we shall call quarter-period throughout this paper. In reality, the typical time scale would be given by the rate-limiting step in the mechanochemical cycle of the motor. (In the case of myosin V it is ADP release.) The spatial period is 3, thus the potential has three independent values, $V_a(\tau)$, $a = 0, 1, 2$, with $V_a(\tau) = V_a(\tau - 4t)$. We fix $V_0(\tau) = 0$ and let the other two evolve in a step-wise pattern

$$V_1(\tau) = V_2(\tau + t) = \begin{cases} 1 & \text{for } 0 < \tau < t, \\ 1 + 2(1 - \lfloor\tau\rfloor/t) & \text{for } t < \tau < 2t, \\ -1 & \text{for } 2t < \tau < 3t, \\ -1 - 2(1 - \lfloor\tau\rfloor/t) & \text{for } 3t < \tau < 4t \end{cases} \tag{2}$$

where $\lfloor\tau\rfloor$ stands for integer part of τ. We can see that the potential V_2 is delayed with respect to V_1 by one quarter period. This implies that the potential $V(x,\tau)$ forms a kind of a "travelling wave" which induces the preferential direction of the diffusive movement of particles. If the delay between V_1 and V_2 was reversed, the direction of the "travelling wave" would be reversed too and so would be the average current. Hence the name "reversible ratchet" for this kind of setup. It is consistent with the power-stroke mechanism [35] which is responsible for most of the movement of motor proteins.

Admittedly unrealistic feature is the synchronous change of potential $V(x,\tau)$ at all positions x, which is not correlated with the actual positions of the particles. In fact, each motor particle can be in a different stage of the motor cycle. Here we assume that all of them change their state in parallel, in conformity with the "reversible ratchet" model of [32, 36, 37]. We also do not take into account the fact that the internal state of the motor is strongly correlated with its position in space.

The second part of the potential in (1) comes from the uniform and static external force F against which a useful work is done. This is the load imposed on the motor.

Finally, the third term in (1) describes the repulsive on-site interaction between particles, with strength $g \geq 0$. The j-th particle feels the presence of the other particles, so we denote

$n_j(x,\tau) = \sum_{i=1}^{N} \overline{\delta}(i-j)\delta(x-x_{i\tau})$ the number of these particles on site x at time τ. (We use $\delta(a-b)$ for Kronecker delta and $\overline{\delta}(a-b) = 1-\delta(a-b)$.)

Contrary to the models of [46–48], we allow more particles on a site, thus deviating from the principles of exclusion processes. Our motivation for this choice is the movement of hard-core particles in narrow two- or three-dimensional channels, where the particles may bypass each other and thus pose obstacles of finite strength, rather than impenetrable barriers to each other. Similar situation may occur also in biological systems, if the motors move along closely spaced parallel tracks, or perhaps even on the same fibre, as may be the case of myosin molecules on an actin filament. The true interaction in these cases is hard-core repulsion, but spatial constraint to the movement of other particles may be effectively considered as finite repulsive potential. Certainly, we recover exclusion-process behaviour in the limit $g \to \infty$.

2.2 Movement of Particles

The configuration X_τ evolves in discrete time. In each discrete tick only one particle (at most) is allowed to move. Since we shall measure the average current, i.e. average distance travelled in a unit of time, per particle, the time should be rescaled appropriately with the number of particles N. This leads to the tick length equal to $1/N$. Therefore, the discrete time instants are $\tau = 0, 1/N, 2/N, \ldots$.

The evolution is a Markov process governed by a master equation. In order to write the master equation in a compact way, let us denote $X(i+)$ and $X(i-)$ the configurations which differ from the configuration X only by the shift of i-th particle one step rightwards and leftwards, respectively. We can write explicitly for these shifted configurations $x_j(i\pm) = (x_i \pm 1)\delta(i-j) + x_j\overline{\delta}(i-j)$. As we allow only one particle hopping to its nearest neighbour site, the two configurations $X(i\pm)$ are the only states to which the system may evolve from the configuration X. Conversely, these two are also the only ones from which the configuration X can be reached.

Then, the master equation can be written as

$$P(X,\tau+1/N) = \frac{1}{N}\sum_{i=1}^{N}\sum_{\sigma=\pm}\Big(W(X(i\sigma)\to X,\tau)P(X(i\sigma),\tau) - W(X\to X(i\sigma),\tau)P(X,\tau)\Big). \tag{3}$$

The transition probabilities $W(X(i\sigma)\to X,\tau)$ must satisfy the detailed balance condition. There are many possible choices which obey this requirement. We found most convenient the following one

$$W(X\to X(j\pm),\tau) = \frac{1}{2}\Big[1+\exp\Big(\beta(U_j(x_{j\tau}\pm 1,\tau) - U_j(x_{j\tau},\tau))\Big)\Big]^{-1}. \tag{4}$$

For convenience, we define the temperature T so that $\beta = 270/T$.

Somewhat awkward definition of system dynamics was chosen so that it exactly reproduces the algorithm of numerical simulations of Ref. [60]. Indeed, in plain words we can say that at each integer time step we select N times a particle randomly and let it make one step leftwards or rightwards in the potential (1). Therefore, on average each particle moves once per unit time, but for large N the probability that it moves exactly k times is given by the Poisson distribution $P(k) = 1/(\mathrm{e}k!)$.

2.3 Mapping on Time-Independent Potential Problem

Without interaction, $g = 0$, the movement of $N \to \infty$ particles in time-dependent potential can be formulated as one-particle problem with time-independent transition probabilities by the usual "stroboscopic" trick. First, it is sufficient to work at integer times τ. We also exploit the spatial periodicity of the potential $V(x)$, with period 3, and define the vector of probabilities with $12t$ components

$$P^R(x + 3\tau, \tau') = \sum_{x'=0}^{L/3-1} P(x + 3x', \tau' + \tau) \tag{5}$$

where now τ' is an integer multiple of $4t$, $x \in \{0, 1, 2\}$, and $\tau = 0, 1, \ldots, 4t - 1$. Its evolution is described by the master equation

$$P^R(\tau' + 4t) = W^R P^R(\tau') \tag{6}$$

and the matrix W^R is composed of 3×3 blocks

$$W^R = \begin{pmatrix} 0 & 0 & \ldots & 0 & W(4t-1) \\ W(0) & 0 & \ldots & 0 & 0 \\ 0 & W(1) & \ldots & & 0 \\ \vdots & & & & \vdots \\ 0 & & \ldots & W(4t-2) & 0 \end{pmatrix}. \tag{7}$$

Each non-zero block $W(\tau')$ corresponds to movement of one particle in time-independent potential. One hop of the particle in such potential is governed by the probabilities (4) which are arranged in 3×3 matrix

$$W_1(\tau) = \begin{pmatrix} 1 - W_1(0+,\tau) - W_1(0-,\tau) & W_1(1-,\tau) & W_1(2+,\tau) \\ W_1(0+,\tau) & 1 - W_1(1+,\tau) - W_1(1-,\tau) & W_1(2-,\tau) \\ W_1(0-,\tau) & W_1(1+,\tau) & 1 - W_1(2+,\tau) - W_1(2-,\tau) \end{pmatrix} \tag{8}$$

where, in the non-interacting case, the transition probabilities (4) simplify to

$$W_1(x\pm,\tau) = \frac{1}{2}\Big[1 + \exp\Big(\beta(V_{x\pm1 \bmod 3}(\tau) - V_x(\tau) \pm F)\Big)\Big]^{-1}. \tag{9}$$

As the actual number of steps the particle makes is Poisson-distributed with average 1, we have $W(\tau) = \sum_{k=0}^{\infty} \frac{1}{ek!}(W_1(\tau))^k = \exp(W_1(\tau) - 1)$.

2.4 Quantities of Interest

The stationary state P^R_{stac} of the process (6) then yields the average stationary current

$$J = \sum_{x=0}^{2}\sum_{y=0}^{2}\sum_{\tau=0}^{4t-1}\Big(W_1(y+,\tau) - W_1(y-,\tau)\Big) \times \Big[\frac{\exp(W_1(\tau) - 1) - 1}{W_1(\tau) - 1}\Big]_{yx} P^R_{\text{stac}}(x + 3\tau). \tag{10}$$

The middle factor containing the exponential of $W_1 - 1$ stems from summing over contributions from particle making k steps, for all positive k with Poisson distribution.

Similarly, the input energy is

$$E_{\rm in} = \sum_{x=0}^{2} \sum_{\tau=0}^{4t-1} \Big(V_x(\tau) - V_x(\tau - 1) \Big) P^R_{\rm stac}(x + 3\tau) \tag{11}$$

and hence the efficiency $\eta = JF/E_{\rm in}$.

3 Mean-Field Approximation

When the interaction is switched on, we can still define the one-particle probability vector as in (5), but it is not any more subject to the Markov process governed by a master equation like (6). However, for small enough g we can expect that the interaction-induced correlations will be weak and we can proceed by an effective one-particle approximation. We shall retain all machinery of the "stroboscopic" approach exposed in the last section, i.e. the equations (6) to (11), except the expression (9) which will be replaced by an approximative one.

3.1 Mean-Field One

There are several ways how to implement a one-site, or mean-field approximation. The first one, investigated in part already in our previous work [60], neglects totally the fluctuations in the particle density. The term $gn_j(x, \tau)$ in (1) was replaced by $g\rho P^R(x + 3\tau)$. (We assume normalisation $\sum_{x=0}^{2} P^R(x + 3\tau) = 3$ for all τ.) If there are only few particles around, movements of any single particle bring about big relative density fluctuations. Therefore, the approximation should be appropriate at high particle densities $\rho = N/L$, while keeping the product $g\rho$ small. Indeed, this expectation was confirmed in [60]. We shall denote this approximation by the acronym MF1 and it amounts taking

$$W_1(x\pm, \tau) = \frac{1}{2} \Big\{ 1 + \exp \Big[\beta \Big(V_{x\pm 1 \bmod 3}(\tau) - V_x(\tau) \pm F + g\rho \big(P^R(x \pm 1 \bmod 3 + 3\tau) - P^R(x + 3\tau) \big) \Big) \Big] \Big\}^{-1} \tag{12}$$

in place of the expression (9). Note that this expression depends on interaction and density only through the product $g\rho$. This is in contrast with simulations, unless $g\rho \to 0$, as we have shown in [60].

3.2 Mean-Field Two

One can partially take into account the one-site density fluctuations, while keeping different sites uncorrelated. Here we have to make a hypothesis about the probability distribution $P_1(n; x, \tau)$ of number of particles at site x in time τ. If we had the stationary solution of (6) at our disposal, we could equate the average number of particles

$$\overline{n}(x, \tau) \equiv \sum_n n P_1(n; x, \tau) = \rho P^R_{\rm stac}(x + 3\tau) \tag{13}$$

but this is still too little information to infer the distribution. Thus, as the favourite choice, we assume $P_1(n; x, \tau)$ to be a Poisson distribution with average $\lambda(x, \tau) = \rho P^R_{\mathrm{stac}}(x + 3\tau)$. Hence, in the approximation we denote MF2 we have, instead of (9), the expression

$$W_1(x\pm, \tau) = \frac{1}{2}\sum_{n=0}^{\infty}\sum_{n'=0}^{\infty} \mathrm{e}^{-\lambda(x,\tau)-\lambda(x\pm 1 \bmod 3,\tau)} \frac{\lambda^n(x,\tau)\lambda^{n'}(x \pm 1 \bmod 3, \tau)}{n!n'!} \times \left\{1 + \exp\left[\beta\Big(V_{x\pm 1 \bmod 3}(\tau) - V_x(\tau) \pm F + g(n' - n)\Big)\right]\right\}^{-1}. \quad (14)$$

3.3 Mean-Field Three

We can further improve this approximation in two directions. First, we should take into account the fact that if we calculate the probability of particle hopping from x to $x \pm 1$, the densities of particles at x and $x \pm 1$ are influenced by the presence of at least one particle at x. Indeed, this is the particle which will try to hop. We shall see later how this constraint is implemented in the calculation. This way we partially take into account not only one-site fluctuations, but also the correlations between neighbour sites.

Second, we can choose more refined assumption on the on-site probability distribution of particle numbers, replacing the simple-minded Poisson by something better. Indeed, the Poisson distribution implicitly assumes independence of particles. It the particles repel each other, the actual distribution for large number of particles must fall lower the Poisson. We found that the following two-parametric modification of the Poisson distribution gives good results

$$P_1(n; \lambda, \widetilde{\lambda}) = \begin{cases} 0 & \text{for } n < m, \\ a & \text{for } n = m, \\ b\widetilde{\lambda}^n/n! & \text{for } n > m \end{cases} \quad (15)$$

where the constants a and b are fixed by the normalisation $\sum_n P_1(n) = 1$ and average $\sum_n n P_1(n) = \lambda$. With this prescription, the average number of particles is λ, but for $n > m$ the distribution behaves like a Poisson distribution with another parameter $\widetilde{\lambda} < \lambda$, taking into account the repulsion. For the parameter m, we take the smallest non-negative integer consistent with the obvious requirement $P_1(n) \geq 0$.

In the prescription (15) we dropped the dependence on space and time. It enters into the distribution $P_1(n)$ through the two parameters λ and $\widetilde{\lambda}$. Let us see now how they are found.

First, we should notice that in calculating the single hop probability $W_1(x\pm)$, we need separately the distribution $P_1(n; \lambda(y), \widetilde{\lambda}(y))$ of the number of particles at point $y = x \pm 1$ to which the hop is directed, and the distribution $P_1(n; \lambda(x), \widetilde{\lambda}(x))$ of the number of particles other than the hopping particle at the point x, from which the hop is performed. Without interaction, these two distributions are not influenced by the fact that there must be a particle at the point x. Certainly, this is the particle which is about to hop, so it must be there. When we switch on the interaction, the things change. It is natural to consider the following situation. We put an extra fixed particle at site x and calculate the stationary one-particle probability vector $P^R_{\mathrm{stac}|x}$ as before, where the symbol $|x$ we added in the subscript indicates that the probability is calculated provided that an extra particle is located at x, thus modifying the potential locally. Similarly, we can add two particles at two points x_1 and x_2 and again calculate the stationary one-particle probability vector $P^R_{\mathrm{stac}|x_1x_2}$. For our purposes it is enough to suppose that either $x_1 = x_2$, i.e. there are two extra particles at the same point, or $|x_1 - x_2| = 1$, i.e. x_1 and x_2 are neighbours.

Then, we could calculate the true one-particle probability vector P^R_{stac}, if we knew the results obtained for $P^R_{\mathrm{stac}|x}$ and $P^R_{\mathrm{stac}|x_1x_2}$. Indeed in the one-hop probability

$$W_1(x\pm,\tau) = \frac{1}{2}\sum_{n=0}^{\infty}\sum_{n'=0}^{\infty} P_1(n;\lambda(x,\tau),\widetilde{\lambda}(x,\tau))\,P_1(n';\lambda(x\pm,\tau),\widetilde{\lambda}(x\pm,\tau)) \times\left\{1+\exp\left[\beta\Big(V_{x\pm1\mathrm{mod}3}(\tau)-V_x(\tau)\pm F+g(n'-n)\Big)\right]\right\}^{-1} \tag{16}$$

we can choose

$$\begin{aligned}\lambda(x,\tau) &= \rho P^R_{\mathrm{stac}|x}(x+3\tau),\\ \lambda(x\pm,\tau) &= \rho P^R_{\mathrm{stac}|x}(x\pm1+3\tau).\end{aligned} \tag{17}$$

For the second parameter of the distribution, we choose

$$\begin{aligned}\widetilde{\lambda}(x,\tau) &= \rho P^R_{\mathrm{stac}|xx}(x+3\tau),\\ \widetilde{\lambda}(x\pm,\tau) &= \rho P^R_{\mathrm{stac}|x}(x\pm1+3\tau)\frac{P^R_{\mathrm{stac}|x\pm1x\pm1}(x\pm1+3\tau)}{P^R_{\mathrm{stac}|x\pm1}(x\pm1+3\tau)}.\end{aligned} \tag{18}$$

This choice takes into account the effect of the reduction of the probability of higher occupation of one site, due to repulsive interaction.

But now the problem of calculating P^R_{stac} is reduced to the problem of obtaining $P^R_{\mathrm{stac}|x}$ and $P^R_{\mathrm{stac}|x_1x_2}$. In principle we could continue further this way, adding three, four, etc. extra particles at various positions and from the known $P^R_{\mathrm{stac}|x_1x_2\ldots x_{n+1}}$ and $P^R_{\mathrm{stac}|x_1x_2\ldots x_n}$ we can deduce the necessary values of λ and $\widetilde{\lambda}$ needed for the calculation of $P^R_{\mathrm{stac}|x_1x_2\ldots x_{n-1}}$ according to formulae analogous to (17) and (18). Of course, in practice we must terminate this recursive chain somewhere. In this work we break the chain just after adding two particles. So, for example when we calculate the spatial distribution of particles in presence of one extra particle at site y, which is $P^R_{\mathrm{stac}|y}$, we use the following parameters in the hopping probability (16)

$$\begin{aligned}\lambda(x,\tau) &= P^R_{\mathrm{stac}|xy}(x+3\tau),\\ \lambda(x\pm,\tau) &= P^R_{\mathrm{stac}|xy}(x\pm1+3\tau),\\ \widetilde{\lambda}(x,\tau) &= P^R_{\mathrm{stac}|xy}(x+3\tau)\frac{P^R_{\mathrm{stac}|xx}(x\pm1+3\tau)}{P^R_{\mathrm{stac}|x}(x\pm1+3\tau)},\\ \widetilde{\lambda}(x\pm,\tau) &= P^R_{\mathrm{stac}|xy}(x\pm1+3\tau)\frac{P^R_{\mathrm{stac}|x\pm1x\pm1}(x\pm1+3\tau)}{P^R_{\mathrm{stac}|x\pm1}(x\pm1+3\tau)}.\end{aligned} \tag{19}$$

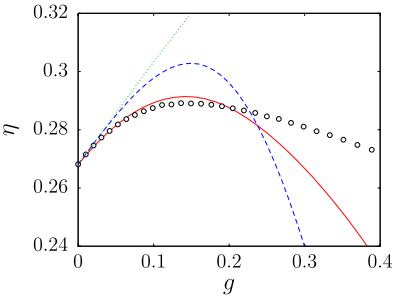

Fig. 1 Efficiency of the reversible ratchet as found by numerical simulations (○), and the three versions of the mean-field approximation, MF1 (*dotted line*), MF2 (*dashed line*) and MF3 (*solid line*). The quarter-period is $t = 16$, particle density is $\rho = 0.3$, temperature $T = 30$ and external load $F = 0.1$

Similarly, for the calculation of the particle probability in presence of two extra particles, i.e. $P^R_{\text{stac}|yz}$, we use

$$\begin{aligned}
\lambda(x,\tau) &= P^R_{\text{stac}|yz}(x+3\tau),\\
\lambda(x\pm,\tau) &= P^R_{\text{stac}|yz}(x\pm 1+3\tau),\\
\widetilde{\lambda}(x,\tau) &= P^R_{\text{stac}|yz}(x+3\tau)\frac{P^R_{\text{stac}|xx}(x\pm 1+3\tau)}{P^R_{\text{stac}|x}(x\pm 1+3\tau)},\\
\widetilde{\lambda}(x\pm,\tau) &= P^R_{\text{stac}|yz}(x\pm 1+3\tau)\frac{P^R_{\text{stac}|x\pm 1x\pm 1}(x\pm 1+3\tau)}{P^R_{\text{stac}|x\pm 1}(x\pm 1+3\tau)}.
\end{aligned} \tag{20}$$

This is the ultimate of the approximations used here and we denote it by acronym MF3.

3.4 Comparison

We can compare the three approximations with the results of the numerical simulation in a typical situation shown in Fig. 1. MF1 is clearly the worst one. However, in the limit of very weak interaction, $g \to 0$, all three approximations seem to reproduce exactly the derivative $\lim_{g\to 0} \frac{\mathrm{d}\eta}{\mathrm{d}g}$. So, the bare existence of the effect of efficiency increase is reproduced in all the approximations tried here, including the simplest MF1.

The second approximation, MF2, grasps also the location of the maximum of the efficiency, but the value at the maximum does not agree quantitatively very well. On the other hand, MF3 agrees also quantitatively well with the location and height of the maximum and starts to deviate markedly from the simulation results only for interactions larger than about $g \simeq 0.3$. Still, we checked that qualitatively the features of the system are reproduced by the approximation MF3 even for very strong repulsion, up to the regime where the limit $g \to \infty$ is effectively reached. Therefore, in the rest of the paper we shall use solely the approximation MF3.

4 Efficiency and Current

4.1 Dependence on the Driving Speed

The behaviour of the motors depends on how fast the external potential changes, i.e. on the quarter-period t. When it increases, the average driving weakens and the current diminishes. At the same time, the process approaches the adiabatic limit, which should imply larger

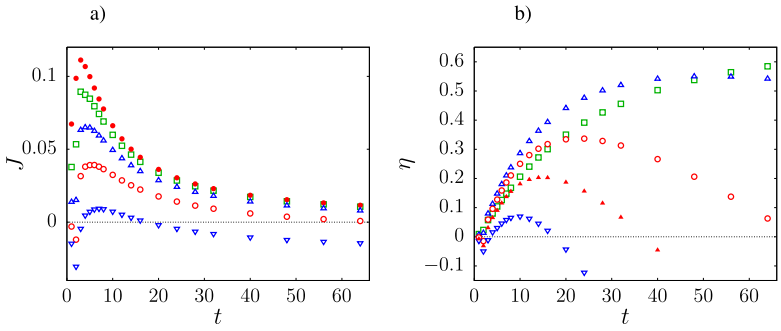

Fig. 2 Dependence of the current (**a**) and efficiency (**b**) on the quarter-period. The density is $\rho = 0.5$, temperature $T = 30$, interaction $g = 0.1$. The load is $F = 0$ (●), $F = 0.1$ (□), $F = 0.2$ (△), $F = 0.3$ (○), $F = 0.35$ (▲), and $F = 0.4$ (▽)

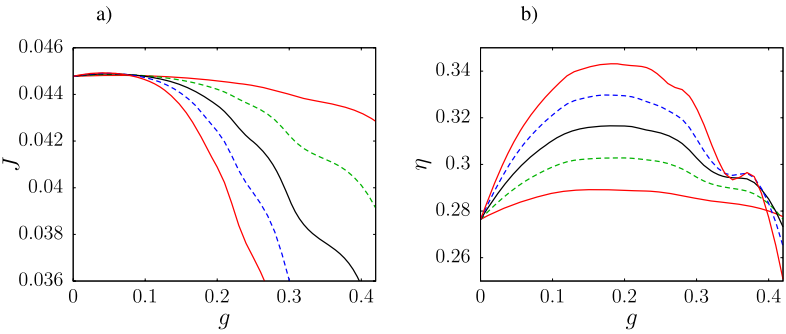

Fig. 3 Dependence of the current (**a**) and efficiency (**b**) on interaction strength, for several densities. The quarter-period is $t = 16$, temperature $T = 10$, load $F = 0.1$, and density (*from top-right to bottom-left in the panel* (**a**), *from bottom to top in the panel* (**b**)) $\rho = 0.1$ (*solid line*), 0.2 (*dashed*), 0.3 (*solid*), 0.4 (*dashed*), 0.5 (*solid*)

efficiency. We can see in Fig. 2 that this expectation is exactly fulfilled in our model of interacting motors. The current diminishes but efficiency grows when the dynamics of the external potential is slowed down. At certain value of the load, the sign of the current reverses and therefore also the efficiency becomes negative. So, at finite load, the efficiency develops a maximum at finite value of t.

4.2 Enhancement of Efficiency

The main result concerns the dependence of the efficiency on interaction strength. To see that, we show in Fig. 3 both current and efficiency as functions of the interaction parameter g. There is a pronounced maximum of efficiency for finite value of the interaction, while the current behaves differently. When the interaction is increased, the current first stays practically constant and about the same value of the interaction, where the maximum of the efficiency occurs, the current starts decreasing rather sharply. We show in Fig. 5a that the presence of the maximum in efficiency is combination of two effects. The first is the initial plateau of current as function of g, the second is the decrease in the input energy per unit time E_{in}. This means that moderately strong repulsive interaction induces collective effects, which results in larger energetic efficiency of the motors.

The increase of the efficiency is larger for larger densities, as seen again in Fig. 3. This agrees with the results of numerical simulations presented in [60]. Note that the naive approximation MF1 does not possess this feature, as all quantities in this approximation depend only on the product $g\rho$ and all curves in Fig. 3 would collapse into one if plotted as functions of $g\rho$.

4.3 At Strong Interaction

Although the mean-field approximation gives only qualitatively correct results if the interaction is stronger than about $g \simeq 0.3$, we can still obtain useful qualitative results. In Fig. 4a we show the efficiency as a function of g for several values of the external load F. For some F (in our figure it occurs for $F = 0.34$), a double current reversal can be observed. When the interaction is small, the current (i.e. also the efficiency) is positive. When we increase the interaction beyond certain limit, the orientation of the current reverses, which is manifested by efficiency changing sign. But if we further increase the interaction strength, the current reverses again and approaches a positive limit for g above about $g \simeq 2$. This limit can be considered as the value corresponding to the exclusion process limit $g \to \infty$.

In Fig. 4b we plot the total current $J_{\text{tot}} = \rho J$ in this exclusion limit as a function of density. It is well known that in the ASEP model, the mean-field result for this current $J_{\text{tot}} = \rho(1-\rho)$ is exact. It means, for example, that the maximum is reached at density $1/2$. Fig. 4b shows that the reversible ratchet we are studying here behaves quite differently. The maximum is at much lower densities and, most importantly, the current reversal phenomenon, discussed already in the previous paragraph, leads to negative current for densities above certain critical value $\rho_c < 1$. In our case, the current changes sign about $\rho_c \simeq 0.34$. This fact makes the ratchet model with exclusion interaction substantially different from the ASEP model.

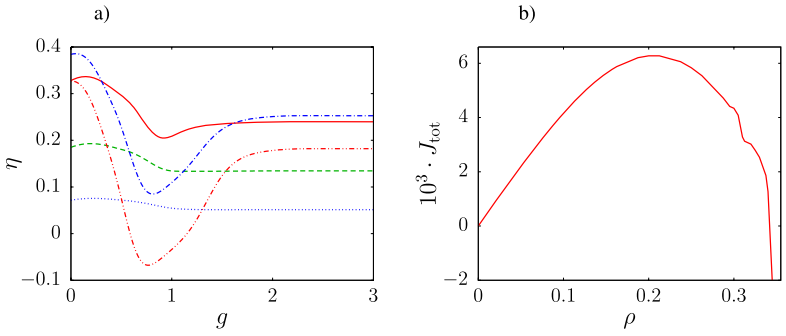

Fig. 4 (**a**), dependence of the efficiency on interaction up to effectively infinite interaction strengths. The density is $\rho = 0.1$, temperature $T = 30$, quarter-period $t = 16$, and load $F = 0.02$ (*dotted line*), $F = 0.06$ (*dashed*), 0.14 (*solid*), 0.28 (*dot-dashed*) and 0.34 (*dot-dot-dashed*). (**b**) Dependence of the total particle current on the density, for temperature $T = 30$, quarter-period $t = 16$, zero load and interaction $g = 3$ (i.e. effectively infinite)

5 Work Fluctuations

5.1 Magnitude

The work performed by a single motor particle within given time interval $\Delta\tau$ is proportional to the displacement Δx of the particle during that time. The work is a random variable and we can study its fluctuations through the probability distribution of the displacements $P(\Delta x)$. (We drop the dependence on the time $\Delta\tau$ from the notation, as it will be clear enough from the context.) The immediate motivation for such study is the question, whether the increase of efficiency of the motor is connected to suppression of fluctuations, as it would be in the case of traditional heat engines.

We show in Fig. 5b the distribution of distances travelled by the particle during relatively long time, $\tau = 1000t$, i.e. 250 periods of the external driving potential. We can see that the distribution is not Gaussian. First, it is composed of two separate branches, depending on the congruence class with respect to spatial periodicity of the external potential. The higher branch corresponds to $\Delta x \equiv 0 \bmod 3$, the lower one to all other Δx. Therefore, it is significantly more probable that after integer number of periods the particle ends in spatially equivalent position than elsewhere.

But even if we take both branches separately, they resemble Gaussians only in the centre of the distribution. The tails are clearly skewed, favouring the backward steps over the forward ones.

However, the most interesting observation comes from the comparison of the distribution without interaction, $g = 0$, and with interaction, $g = 0.12$, where all other parameters are equal. We checked that of the two, the interacting case exhibits enhanced efficiency. Looking at Fig. 5b we can see that the width of the distribution is larger in the interacting case, so the work fluctuations are bigger, rather than smaller, in the more efficient state. We have already remarked that the increase of efficiency is accompanied by decrease of energy input, as seen in Fig. 5a. Hence, from Figs. 5a, b combined we conclude that the effect of enhanced efficiency has energetic, rather than entropic origin. This means that the efficiency issue in Brownian motors is distinct from the situation in equilibrium thermal engines.

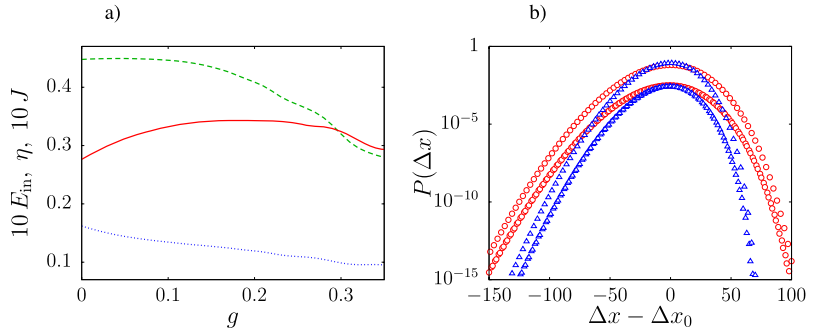

Fig. 5 Source of the increase of the efficiency. (**a**) Dependence of current (*dashed line*), efficiency (*solid line*) and input energy (*dotted line*) on interaction strength. The density is $\rho = 0.5$, temperature $T = 10$, quarter-period $t = 16$, load $F = 0.1$. (**b**) Show the distribution of displacement after time $\Delta\tau = 1000t$, for $t = 16$, $T = 30$, $\rho = 0.5$, $F = 0.1$ and interaction $g = 0$ (△) and $g = 0.12$ (○). The distributions are plotted relative to the position of the maximum Δx_0

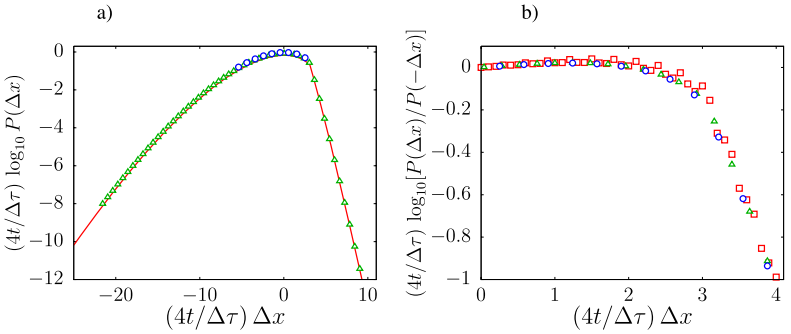

Fig. 6 (**a**) Large deviation function for the particle displacement. The time distances are, *from the left to the right*, $\Delta\tau = 40t$ (*line*), $100t$ (△), $400t$ (○). (**b**) Odd part of the large deviation function, for time distances $\Delta\tau = 40t$ (□), $100t$ (△), $400t$ (○). *In both panels*, the parameters are $\rho = 0.5$, $T = 30$, and $t = 16$ $g = 0.1$ and $F = 0.4$

5.2 Large Deviations and Symmetry

Gaussian or not, the distribution of displacements $P(\Delta x)$ is expected to converge, when appropriately scaled, to a function which describes large deviations from the average value

$$l(\xi) = \lim_{\Delta\tau\to\infty} \frac{1}{\Delta\tau} \ln P(\xi\,\Delta\tau) \tag{21}$$

where $\xi = \Delta x/\Delta\tau$. We can see in Fig. 6a that limit as found numerically within our mean-field approximation. We can see that the function is indeed very far from a Gaussian, reflecting the far-from-equilibrium nature of the ratchet transport. The backward skew is very pronounced.

In the last decade, there was a surge of interest in fluctuation symmetries. In the non-equilibrium systems with time-independent driving, the entropy production satisfies a simple but highly non-trivial fluctuation theorem (FT) [63–65]. Formulated in words, it states that the odd part of the large deviation function for entropy production is a linear function. There are cases, when the entropy production is proportional to the current, where FT holds also directly for the large deviations of the displacement [66–68]. Essentially these are the cases where particles are allowed to hop only to the nearest-neighbour positions on a one-dimensional lattice. We were interested how far the ratchet model investigated here is from such situation, so we plotted in Fig. 6b separately the odd part of the large deviation function. As we can see, it is not linear. It is no surprise, in fact, as the driving in the ratchet is time-dependent. This could be given a simple interpretation, that the current is not proportional to the entropy production, because at different times a single particle hopping bears different entropy change. One could proceed by defining the ensemble of currents, one for each instant within the time-period separately. Then, one would expect that the FT would hold for inversion of all these current simultaneously, in the spirit of [69], although it could well be that the interaction spoils this property. Alas, such study would be impractical in our case, because the number of currents would be too large. In fact, we would need to work with joint probability distribution of $4t$, i.e. in our calculations typically 64, variables.

6 Conclusions

We investigated the applicability of several mean-field approximation schemes for a model of interacting Brownian motors. We selected the method based on the assumption of modified Poisson distribution for the number of particles simultaneously present at one site. The method was shown to give quantitatively reasonable agreement for interaction strengths up to about $g \simeq 0.3$. Beyond that limit the behaviour still remains qualitatively valid. We investigated the effect of the enhancement of the efficiency of the motors due to interactions. Calculating the energetic balance and work fluctuations we concluded that the effect of enhanced efficiency is caused entirely by the lowered energy input and not by the effect of lower fluctuations. Indeed, fluctuations are increased, rather than decreased, by the interactions. This is in contrast with the standard situation found in equilibrium engines.

We calculated also the properties of the model for strong interaction, where it approaches the hard-core repulsion. The efficiency and current approaches a non-zero limit for $g \to \infty$ (actually the limit value is reached already at $g \simeq 3$). The current-density diagram at such large interaction exhibits significantly different behaviour than the ASEP model, showing that the results for ASEP cannot be directly translated into the properties of ratchets. Most notable difference is the current reversal effect, which implies that not only the absolute size, but also the orientation of the current depends on the interaction strength and on the density.

We also calculated the large deviation function, which is far from Gaussian, manifesting the far-from-equilibrium nature of the particle transport. The question of fluctuations symmetries of the ratchet current in this type of molecular motor remains unclear. There are works suggesting the validity of the fluctuation theorem in some ratchets, if the time-dependent driving is periodic and obeys time-reflection symmetry at least at one point within the period [69–74]. Our ratchet does not possess this property. We showed that the displacement (i.e. current) fluctuations do not obey the fluctuation theorem, but proper analysis of this question requires further detailed study.

The symmetry of the ratchet current was investigated relatively recently in [75], but our ratchet differs from the types investigated there by seemingly minor point that the ratchet potential can be in more than two states. Therefore, the ratchet symmetry operation is not a simple reflection as in [75] and the results presented there cannot be easily translated into our case.

Acknowledgements I gladly acknowledge inspiring discussions with P. Chvosta, K. Netočný, and R. Harris. This work was carried out within the project AV0Z10100520 of the Academy of Sciences of the Czech republic and was supported by the Grant Agency of the Czech Republic, grant no. 202/07/0404.

References

1. Ajdari, A., Prost, J.: C. R. Acad. Sci. Paris, Sér. II **315**, 1635 (1992)
2. Magnasco, M.O.: Phys. Rev. Lett. **71**, 1477 (1993)
3. Bartussek, R., Hänggi, P., Kissner, J.G.: Europhys. Lett. **28**, 459 (1994)
4. Jülicher, F., Ajdari, A., Prost, J.: Rev. Mod. Phys. **69**, 1269 (1997)
5. Astumian, R.D.: Science **276**, 917 (1997)
6. Kolomeisky, A.B., Widom, B.: J. Stat. Phys. **93**, 633 (1998)
7. Reimann, P., Hänggi, P.: Appl. Phys. A **75**, 169 (2002)
8. Reimann, P.: Phys. Rep. **361**, 57 (2002)
9. Hänggi, P., Marchesoni, F., Nori, F.: Ann. Phys. (Leipzig) **14**, 51 (2005)
10. Lipowsky, R., Chai, Y., Klumpp, S., Liepelt, S., Müller, M.J.I.: Physica A **372**, 34 (2006)
11. Klumpp, S., Lipowsky, R.: Proc. Natl. Acad. Sci. USA **102**, 17284 (2005)
12. Wang, H., Elston, T.C.: J. Stat. Phys. **128**, 35 (2007)

13. Lipowsky, R., Liepelt, S.: J. Stat. Phys. **130**, 39 (2008)
14. Svoboda, K., Block, S.M.: Cell **77**, 773 (1994)
15. Wang, H., Oster, G.: Nature **396**, 279 (1998)
16. Schliwa, M. (ed.): Molecular Motors. Wiley-VCH, New York (2003)
17. Schliwa, M., Woehlke, G.: Nature **422**, 759 (2003)
18. Carter, N.J., Cross, R.A.: Nature **435**, 308 (2005)
19. Kolomeisky, A.B., Fisher, M.E.: Annu. Rev. Phys. Chem. **58**, 675 (2007)
20. Matthias, S., Müller, F.: Nature **424**, 53 (2003)
21. Kettner, C., Reimann, P., Hänggi, P., Müller, F.: Phys. Rev. E **61**, 312 (2000)
22. Hänggi, P., Marchesoni, F.: arXiv:0807.1283 (2008)
23. Blythe, R.A., Evans, M.R.: J. Phys. A: Math. Theory **40**, R333 (2007)
24. Wang, H., Oster, G.: Europhys. Lett. **57**, 134 (2002)
25. Jülicher, F., Prost, J.: Phys. Rev. Lett. **75**, 2618 (1995)
26. Sekimoto, K.: cond-mat/9611005
27. Sekimoto, K.: J. Phys. Soc. Jpn. **66**, 1234 (1997)
28. Kamegawa, H., Hondou, T., Takagi, F.: Phys. Rev. Lett. **80**, 5251 (1998)
29. Parrondo, J.M.R., De Cisneros, B.J.: Appl. Phys. A **75**, 179 (2002)
30. Qian, H.: Phys. Rev. E **69**, 012901 (2004)
31. Asfaw, M., Bekele, M.: Phys. Rev. E **72**, 056109 (2005)
32. Parrondo, J.M.R., Planco, J.M., Cao, J.F., Brito, R.: Europhys. Lett. **43**, 248 (1998)
33. Qian, H.: Biophys. Chem. **67**, 263 (1997)
34. Qian, H.: Biophys. Chem. **83**, 35 (2000)
35. Wang, H., Oster, G.: Appl. Phys. A **75**, 315 (2002)
36. Parrondo, J.M.R.: Phys. Rev. E **57**, 7297 (1998)
37. Astumian, R.D., Derényi, I.: Biophys. J. **77**, 993 (1999)
38. Schmiedl, T., Seifert, U.: Europhys. Lett. **83**, 30005 (2008)
39. Lipowsky, R., Klumpp, S., Nieuwenhuizen, T.M.: Phys. Rev. Lett. **87**, 108101 (2001)
40. Klumpp, S., Lipowsky, R.: J. Stat. Phys. **113**, 233 (2003)
41. Parmeggiani, A., Franosch, T., Frey, E.: Phys. Rev. Lett. **90**, 086601 (2003)
42. Klumpp, S., Nieuwenhuizen, T.M., Lipowsky, R.: Biophys. J. **88**, 3118 (2005)
43. Klumpp, S., Lipowsky, R.: Europhys. Lett. **66**, 90 (2004)
44. Scheer, U., Xia, B., Merkert, H., Weisenberger, D.: Chromosoma **105**, 470 (1997)
45. Raška, I., Koberna, K., Malínský, J., Fidlerová, H., Mašata, M.: Biol. Cell **96**, 579 (2004)
46. Greulich, P., Garai, A., Nishinari, K., Schadschneider, A., Chowdhury, D.: Phys. Rev. E **75**, 041905 (2007)
47. Basu, A., Chowdhury, D.: Phys. Rev. E **75**, 021902 (2007)
48. Tripathi, T., Chowdhury, D.: Phys. Rev. E **77**, 011921 (2008)
49. Derrida, B., Domany, E., Mukamel, D.: J. Stat. Phys. **69**, 667 (1992)
50. Derrida, B., Evans, M.R., Hakim, V., Pasquier, V.: J. Phys. A: Math. Gen. **26**, 1493 (1993)
51. Derrida, B.: Phys. Rep. **301**, 65 (1998)
52. Nagel, K., Schreckenberg, M.: J. Phys. I Fr. **2**, 2221 (1992)
53. Derényi, I., Vicsek, T.: Phys. Rev. Lett. **75**, 374 (1995)
54. Derényi, I., Ajdari, A.: Phys. Rev E **54**, R5 (1996)
55. Aghababaie, Y., Menon, G.I., Plischke, M.: Phys. Rev. E **59**, 2578 (1999)
56. Reimann, P., Kawai, R., van den Broeck, C., Hänggi, P.: Europhys. Lett. **45**, 545 (1999)
57. Stukalin, E.B., Kolomeisky, A.B.: Phys. Rev. E **73**, 031922 (2006)
58. Campàs, O., Kafri, Y., Zeldovich, K.B., Casademunt, J., Joanny, J.-F.: Phys. Rev. Lett. **97**, 038101 (2006)
59. Jülicher, F., Prost, J.: Phys. Rev. Lett. **78**, 4510 (1997)
60. Slanina, F.: Europhys. Lett. **84**, 50009 (2008)
61. Kondratiev, Y., Pechersky, E., Pirogov, S.: arXiv:0706.2931 (2007)
62. Cappello, G., Pierobon, P., Symonds, C., Busoni, L., Gebhardt, J.C.M., Rief, M., Prost, J.: Proc. Natl. Acad. Sci. USA **104**, 15328 (2007)
63. Evans, D.J., Cohen, E.G.D., Morriss, G.P.: Phys. Rev. Lett. **71**, 2401 (1993)
64. Gallavotti, G., Cohen, E.G.D.: Phys. Rev. Lett. **74**, 2694 (1995)
65. Kurchan, J.: J. Phys. A: Math. Gen. **31**, 3719 (1998)
66. Lebowitz, J.L., Spohn, H.: J. Stat. Phys. **95**, 333 (1999)
67. Maes, C.: J. Stat. Phys. **95**, 367 (1999)
68. Maes, C., Netočný, K.: J. Stat. Phys. **110**, 269 (2003)
69. Andrieux, D., Gaspard, P.: Phys. Rev. E **74**, 011906 (2006)

70. Seifert, U.: J. Phys. A: Math. Gen. **37**, L517 (2004)
71. Seifert, U.: Europhys. Lett. **70**, 36 (2005)
72. Lau, A.W.C., Lacoste, D., Mallick, K.: Phys. Rev. Lett. **99**, 158102 (2007)
73. Astumian, R.D.: Phys. Rev. E **76**, 020102(R) (2007)
74. Harris, R.J., Schütz, G.M.: J. Stat. Mech. **P07020** (2007)
75. De Roeck, W., Maes, C.: Phys. Rev. E **76**, 051117 (2007)